Variations of Titanium Interactions in Solid State NMR—Correlations to Local Structure

D. Padro,[†,‡] V. Jennings,[†] M. E. Smith,*[,†] R. Hoppe,[§] P. A. Thomas,[†] and R. Dupree*[,†]

Department of Physics, University of Warwick, Coventry, United Kingdom, CV4 7AL, and Institüt für Anorganische Chemie, Universität Giessen, Heinrich Buff Ring 5 88, D-35397 Giessen, Germany

Received: July 10, 2002; In Final Form: October 10, 2002

Direct solid state NMR observation of titanium opens up new possibilities for characterization of many chemical problems. Here, solid state ^{47,49}Ti NMR spectra are reported for a large variety of crystalline ternary and quaternary titanates. A wide range of values for the NMR interaction parameters is observed, with chemical shifts covering ~300 ppm and quadrupole interactions (C_Q) up to 24 MHz. The isotropic chemical shift (δ_{iso}) ranges for TiO_6, TiO_5, and TiO_4 deduced from these samples suggest that NMR can help to determine coordinations in materials where it is unknown, although the strong overlap of these ranges may not allow unequivocal identification in all cases. For TiO_6 units, there is a good correlation of the shear strain of the local TiO_6 unit to C_Q. Similar correlations are found for the much rarer TiO_4 coordination. The correlation of C_Q is generalized through the concept of a distortion index of the local structural unit, which applies to all TiO_x units, including TiO_5. Static NMR data from several samples (e.g., $PbTiO_3$, Sr_2TiO_4) show unequivocally that for some compounds titanium has a significant chemical shift anisotropy, which needs to be included for accurate simulations of static titanium NMR spectra. The electric field gradient determined by NMR does not agree with values previously obtained by perturbed angular correlation. Calculations of the quadrupole parameters using the WIEN97 code, based on the linearized augmented plane wave method, have been carried out for some perovskite- and ilmenite-structured titanates and agree well with the values determined from NMR (i.e., within a few percent), except for the ilmenite form of $CdTiO_3$ where the current structure appears unreliable. The ^{43}Ca NMR spectrum is reported for $CaTiO_3$ showing that $C_Q = 2.15 \pm 0.03$ MHz, $\eta = 0.70 \pm 0.07$, and $\delta_{iso} = 17.2 \pm 1.0$ ppm.

I. Introduction

Increasingly, as ever higher applied magnetic fields become available for NMR spectroscopy, those nuclei with, for example, weak signals, significant quadrupole broadening, or both are becoming ever more tractable. Solid state titanium NMR would open up many problems that are of fundamental importance in chemistry. For example, electroceramics such as $BaTiO_3$ and lead zirconate titanate (PZT) are made up of TiO_6 units, and often, the distortion of the local TiO_6 units influences bulk properties. Other physical properties influenced by the presence of titanium are thermal expansion[1] and refractive index of silicate-based glasses, and from the chemical point of view the catalytic activity of microporous siliceous materials.[2] Other applications of titania-based materials include using them as pigments[3], gas and humidity sensors,[4] photocatalysts,[5] and photovoltaics.[6] In the structural chemistry of bulk, amorphous titanosilicate materials, there is evidence (much of it somewhat indirect) that the preferred coordination of titanium depends in detail on the preparation route. For example, in melt-quenched titanosilicate glasses, TiO_5 units are thought to dominate whereas in amorphous sol−gel-formed materials the structure appears to contain only TiO_6 and TiO_4 units. An approach for direct determination of the coordination of titanium such as solid state titanium NMR would have widespread application to a range of important problems in chemistry and physics.

Despite the range of potential applications and there being two NMR active titanium isotopes (^{47}Ti (nuclear spin $I = 5/2$) and ^{49}Ti ($I = 7/2$)), there has been relatively little solid state titanium NMR published to date.[7] The main experimental difficulty is that both isotopes have moderately large electrical quadrupole moments (Q) in the ratio $^{49}Q/^{47}Q = 0.8179$.[8] It is usually the second-order quadrupolar-broadened central (1/2, −1/2) transition that is observed whose width depends on a factor[9]

$$\frac{Q^2(I(I+1) - 3/4)}{\gamma(2I(2I-1))^2} \tag{1}$$

where γ is the gyromagnetic ratio.

NMR spectra are characterized by a number of tensor interactions with the two most important for titanium being the quadrupole and the chemical shift. A quirk of nature means that the two NMR active titanium isotopes have extremely similar γ values, so that even at 14.1 T their resonance frequencies differ by only ~9 kHz. The second-order quadrupole broadening is dominated by the Q and I factors (eq 1), which for the central transition cause relative broadening of $^{47}\Delta\nu/^{49}\Delta\nu \sim 3.522$. For comparison with ^{27}Al, ^{49}Ti shows a relative broadening that is likely to be at least ~5.6 times larger for sites with the same structural distortion, largely through the effect of the low γ. The difficulty of observation of the relatively broad titanium lines that are typical is exacerbated by the low

* To whom correspondence should be addressed. (M.E.S.) Tel: 0044-24-7652-2380. Fax: 0044-24-7669-2016. E-mail: M.E.Smith.1@warwick.ac.uk. (R.D.) Tel: 0044-24-7652-3403. Fax: 0044-24-7669-2016. E-mail: R.Dupree@warwick.ac.uk.

† University of Warwick.

‡ Present address: Department of Earth Sciences, University of Cambridge, Downing Street, Cambridge, U.K., CB2 3EG.

§ Universität Giessen.

10.1021/jp021583x CCC: $22.00
Published on Web 12/04/2002

natural abundances of only 7.28% for ^{47}Ti and 5.51% for ^{49}Ti, and their small γ values. Spectral interpretation is further complicated by the typical line widths because the small resonance frequency difference between the two isotopes is usually much smaller than the widths of the lines, so that most solid state titanium NMR spectra consist of completely overlapped resonances from the two isotopes. Despite these difficulties, higher applied magnetic fields rapidly alleviate such problems by reducing second-order quadrupole effects, since the line width is proportional to C_Q^2/ν_o (where $C_Q = e^2Qq/(2I(2I-1)$, eq is the electric field gradient (efg), and ν_o is the Larmor resonance frequency) and increasing sensitivity. Hence, with increasingly widespread access to magnetic fields of $\geq$14.1 T, solid state titanium of powdered polycrystalline and amorphous solids now merits serious consideration and investigation.

Solid state ^{47,49}Ti NMR in oxide materials has been reported from the three polymorphs of TiO_2, anatase,[10−12] rutile,[10] and brookite,[13,14] which are all made up of TiO_6 units with the connectivity and relative orientation of these octahedral units distinguishing them. Anatase has the most symmetric site, and hence the smallest efg. Correct excitation conditions on a static sample allow the nested line shapes from both isotopes to be accurately recorded. By magic angle spinning (MAS) anatase, the ^{49}Ti line shape was clearly seen by Dec et al., but with the spinning speeds used, the ^{47}Ti centerband was mixed in with the sidebands from ^{49}Ti.[15] A static powder study recorded the ^{49}Ti resonance of rutile,[10] with the parameters deduced agreeing with those from a single crystal study.[12] Brookite shows shift and quadrupolar parameters intermediate to the other two TiO_2 polymorphs.

Recent studies have reported ^{47,49}Ti solid state NMR spectra from amorphous TiO_2 gels formed by hydrolysis of $Ti(^iOPr)_4$ and heated at 200−700 °C. In a gel heated to 200 °C, which is still amorphous, a surprisingly narrow resonance was observed. This indicated that either the TiO_6 units are quite symmetric or that partial averaging of the quadrupolar parameters is occurring. Heating between 500 and 600 °C produces some complex line shapes, but it was convincingly shown that these line shapes could be decomposed into those of anatase and rutile, with the amount of rutile increasing with heat treatment.[16] Monodisperse crystalline TiO_2 nanoparticles (5−10 nm) obtained by precipitation from $TiCl_4$ in an aqueous solution of HCl have been studied by solid state ^{47,49}Ti NMR.[14] The influence of the size and crystallinity of TiO_2 nanoparticles on the shape of the corresponding ^{47,49}Ti NMR spectra was examined, and the spectra were simulated to quantify the distribution of anatase and rutile. Titanium NMR allowed the changes that occur on annealing at high temperatures to be readily followed. Careful comparison between the phase distribution in these particles, as determined by ^{47,49}Ti NMR and X-ray diffraction (XRD), showed that NMR was better at detecting small amounts of anatase.

Several reports of titanium NMR exist for $BaTiO_3$.[17−20] Narrow ^{49,47}Ti resonances from the cubic phase above the Curie temperature were observed at 7.05 T from powder samples.[17] These signals were lost in the tetragonal phase formed on cooling. Dec et al. showed in a limited range of ABO_3 perovskite materials that the nature of the A cation influences the ^{47,49}Ti NMR spectra with variations of the chemical shift, although they only reported peak positions and not the isotropic chemical shift.[15] In $FeTiO_3$, a broad line with no distinct singularities has been observed. $FeTiO_3$ is paramagnetic at room temperature, and the transferred hyperfine field from the Fe^{3+} produces a large positive shift.[10] $Li_{1+x}Ti_{2-x}O_4$ is a superconductor with a critical temperature of ~12 K. ^{47,49}Ti static NMR spectra were recorded in the range of 160−330 K for the stoichiometric composition ($x = 0$) and as a function of composition ($x < 0.1$).[21]

A recent, more extensive ^{47,49}Ti NMR study of ABO_3 perovskites and ilmenites used static and MAS NMR spectra at 14.1 T to examine further the structural influences on the NMR interaction parameters of some TiO_6 units.[22] Very clear second-order quadrupole-perturbed line shapes could in general be observed, which allowed the interactions to be accurately deduced. C_Q showed a general increase with increasing shear strain with a good correlation. For the perovskites, there was also a reasonable linear correlation of δ_{iso} with the mean Ti−O bond length, although interestingly it was in the opposite direction to that normally observed for nuclei. These initial reports are extremely encouraging but require extension to test the validity of the structural correlations of C_Q. Robust correlations greatly enhance the utility of solid state NMR in providing information about the structure of materials in less well-understood cases. There is also the need to answer the key question about the ability of solid state titanium NMR to distinguish different local coordinations of titanium (i.e., TiO_4, TiO_5, and TiO_6). If NMR could distinguish these different coordinations, it could be applied to many chemically and technologically significant problems. This paper addresses these problems by looking at a wide range of crystalline compounds covering all of the different titanium coordinations for the first time. A combination of MAS and static NMR, in some cases at two applied magnetic fields (8.45 and 14.1 T), allows the NMR interaction parameters (including the chemical shift anisotropy (CSA)) to be accurately deduced for almost all samples so that trends with structure can be studied.

II. Experimental Section

A. Sample Preparation and General Characterization. Some samples were purchased commercially and used without further purification. Others were made by solid state reaction, for example, starting with the metal carbonate and TiO_2 and then heating to 900−1200 °C. All samples were checked for phase purity by powder XRD. All samples used were phase pure except for $ZnTiO_3$ (containing <10% Zn_2TiO_4), Sr_2TiO_4 (<5% $SrTiO_3$), $CaTiSiO_5$ (<5% $CaTiO_3$), and Li_4TiO_4 (<20% Li_2TiO_3). Li_2TiSiO_5 and Na_2TiSiO_5 were manufactured by a sol−gel route[23] starting with stoichiometric amounts of titanium isopropoxide ($Ti(^iOPr)_4$, Aldrich) and tetraethyl orthosilicate (TEOS, Aldrich), which were separately dissolved into dry 2-propanol. The TEOS was prehydrolyzed with water containing HCl as a catalyst. The two solutions were mixed together while stirring followed by adding the requisite amount of finely powdered lithium or sodium carbonate. The mixture was stirred continuously until it gelled. This product was vacuum-pumped to form a dry xerogel. This xerogel was then slowly fired (5 °C/h) up to 900 °C where it was left for 12 h. All of the volatile species were removed by this process leaving a single phase product. Na_4TiO_4 was prepared as described in ref 24.

B. Solid State NMR. Titanium NMR spectra were recorded at 33.80 MHz on a Varian Chemagnetics CMX Infinity 600 spectrometer equipped with a widebore 14.1 T magnet. Static spectra were collected using a Chemagnetics 9.5 mm MAS probe, with some MAS spectra recorded using a Chemagnetics 4 mm T3 probe with a low γ box and sample spinning at up to 17 kHz. Spectral widths of 1 MHz were observed with typically 4 k data points in the FT. Some additional static measurements were carried out at 8.45 T on a CMX Infinity spectrometer operating at a frequency of 20.97 MHz with a 10 mm horizontal

TABLE 1: ^{49}Ti NMR Interaction Parameters for TiO_6 Units in Some Crystalline Materials

compd	structure type	structural ref	C_Q (MHz)	η	δ_{iso} (ppm)
$CaTiO_3$[a]	orthorhombic	30	2.75 ± 0.1	0.70 ± 0.06	-10.5 ± 1
$CdTiO_3$[a]	rhombohedral	31	11.1 ± 0.1	0.10 ± 0.03	30 ± 10
$CdTiO_3$[a]	orthorhombic	32	4.07 ± 0.05	0.40 ± 0.05	40 ± 0.5
$MgTiO_3$[a]	rhombohedral	33	15.52 ± 0.05	0.00 ± 0.05	-15 ± 10
$ZnTiO_3$	rhombohedral	34	14.8 ± 0.2	0.00 ± 0.05	5 ± 10
$Na_{0.5}Bi_{0.5}TiO_3$	rhombohedral	35	5.3 ± 0.5	0.00 ± 0.05	0 ± 10
$CoTiO_3$	rhombohedral	36	14.4 ± 0.1	0.35 ± 0.05	2500
$PbTiO_3$	tetragonal	37	9.45 ± 0.10	0.00 ± 0.05	153 ± 15
				$\Omega = 180 \pm 10$ ppm, $\kappa = 1$	
$BaTiO_3$	tetragonal	38	3.42 ± 0.05	0.00 ± 0.05	112 ± 1
				$\Omega = 22.5 \pm 5$ ppm, $\kappa = -1$	
Sr_2TiO_4	perovskite	39	4.3 ± 0.1	0.00 ± 0.05	26 ± 5
				$\Omega = 120 \pm 10$ ppm, $\kappa = 1$	
Mg_2TiO_4	spinel	40	9.0 ± 0.2	0.50 ± 0.05	-45 ± 10
Zn_2TiO_4	spinel	41	7.4 ± 0.2	0.60 ± 0.05	0 ± 10
Na_2TiO_3		42	7.2 ± 0.2	0.55 ± 0.05	100 ± 10
Li_2TiO_3	distorted NaCl	43	4.6 ± 0.05	0.65 ± 0.05	-10 ± 5
$Ca_4Ti_3O_{10}$,	orthorhombic	44	site 1 2.6 ± 0.05	0.0 ± 0.05	-10 ± 5
			site 2 5.2 ± 0.1	0.5 ± 0.1	-15 ± 10
$Ca_3Ti_2O_7$	orthorhombic	44	5.6 ± 0.1	0.90 ± 0.05	25 ± 10
$Y_2Ti_2O_7$	pyrochlore	45	24.0 ± 0.3	0.00 ± 0.05	-30 ± 15
$Bi_2Ti_2O_7$		46	9.7 ± 0.2	0.75 ± 0.05	-35 ± 15
$CaTiSiO_5$		47	13.8 ± 0.3	0.20 ± 0.05	30 ± 15

[a] Taken from ref 22.

solenoid probe. In all cases, a Hahn spin−echo was applied with extended phase cycling to cancel both probe ringing and direct magnetization from the second pulse. Typically, the sequence used was 1.8 μs (~45°) − τ − 3.6 μs (~90°) with τ in the range of 50−100 μs. Note that the approximate tip angles apply to ^{49}Ti, and because all compounds examined here are in the regime where it is effectively only the central transition that is observed, there is an I dependence of the tip angle.[9] Hence, the effective tip angle will be 0.75 smaller for the ^{47}Ti. For MAS spectra, τ was made an integral number of rotor periods. Recycle delays were in the range of 1−5 s to allow relaxation of the NMR signal, and to obtain a sufficient signal-to-noise, 1000−320 000 transients were coadded. Spectra were formed by either Fourier transforming (FT) from the echo maximum, or if τ was sufficiently long so that both halves of the echo could be acquired completely, the whole echo was transformed after Gaussian smoothing centered on the echo, with the spectrum phased by zeroing the signal in the imaginary channel. To reproduce accurately the line shape for $Y_2Ti_2O_7$, a frequency-stepped echo experiment was undertaken. The spin−echo sequence for quadrupole nuclei (QCPMG) for improved sensitivity introduced by Larsen et al. was also examined.[25,26] Spectra were referenced against a secondary standard of $SrTiO_3$ since this cubic phase has sharp resonances. The ^{49}Ti line was taken as 0 ppm following the suggestion of Bastow et al.[10] as it is a safe, reproducible reference. According to Dec et al.,[14] $SrTiO_3$ is shifted by −843 ppm against ^{49}Ti in liquid $TiCl_4$, the conventional shift standard for titanium, so that the data reported here are readily related back to the primary shift reference.

^{43}Ca NMR data from $CaTiO_3$ were recorded at 14.1 T at a spectral frequency of 40.39 MHz. A 14 mm Chemagnetics probe was used with the sample spinning at 1.45 kHz. One pulse acquisition was applied with a recycle delay of 0.7 s, and 123 k scans were coadded. Dilute aqueous $CaCl_2$ was used as the shift reference at 0 ppm.

C. Computational Analysis. Spectral simulations were undertaken using the dmfit program.[27] The simulations of the central (1/2, −1/2) transition were considered principally second-order quadrupole effects. The fit parameters (C_Q, η, and δ_{iso}) that were able to reproduce best the well-defined spectral features are quoted. In some cases, it was clear that inclusion of CSA effects was required to correctly simulate the central transition (see Results).

Calculations of the efg at the nuclear site were undertaken with the WIEN97 program,[28] which uses a full potential linearized augmented plane wave (LAPW) approach. The atomic coordinates were taken from the crystal structures given in Table 1. The generalized gradient approximation for the exchange correlation potential was used. For this LAPW expansion, the plane wave cutoff parameter ($R_{mt}k_{max}$) ranged from 7 to 9 providing ~1200 plane waves per formula unit. The irreducible part of the Brillouin zone was sampled with 64−256 k points. The G_{max} parameter determining the largest k vector in the Fourier expansion of the charge density was varied between 14 and 20 $(Ry)^{-1/2}$. There were no shape approximations for the potential or the electronic charge density. The calculations were iterated until the value of the efg converged to a value in the range of 0.01−0.001, depending on the complexity of the structure. Our investigations showed that using the standard convergence condition for the energy (to 0.0001 Ry for three consecutive iterations) did not necessarily imply convergence of the efg to a reliable value as well. Therefore, the separate condition for convergence of the efg described above was also applied.

III. Results and Discussion

A. Philosophy of Data Collection and Simulation. To take maximum advantage of structural information available from a nucleus such as titanium, the correct experimental methodology needs to be employed to provide the optimum line shape and resolution. At 14.1 T, there are four well-defined regions of $^{49}C_Q$ (value of C_Q for ^{49}Ti), corresponding to different line widths, for which different experimental approaches are required. These are (i) $^{49}C_Q < 5$ MHz where the line will fully narrow under moderate MAS. When both isotopes narrow, care has to be taken that sidebands from one isotope do not lie on top of the centerband of the other, complicating the simulation. To narrow second-order quadrupole line shapes by MAS, the spinning speed needs to exceed the residual second-order width

of the quadrupole line shape.[9,29] Hence, as C_Q increases, there will be a range where the ^{49}Ti resonance narrows but the ^{47}Ti does not because of the greater second-order quadrupole broadening of the ^{47}Ti resonance. Then, the unnarrowed ^{47}Ti line lies under the sidebands from ^{49}Ti. In this particular regime, the ^{49}Ti line is a much narrower MAS-averaged resonance as compared to the unnarrowed ^{47}Ti line, so that the central part of the ^{49}Ti line appears with much greater amplitude as well. For (ii) 5 MHz < $^{49}C_Q$ < 14 MHz, the ^{49}Ti spectrum will no longer fully narrow under MAS but a complete well-defined static spectrum of both isotopes can be obtained with a normal pulsed echo. The narrower ^{49}Ti resonance is nested within the broader ^{47}Ti line shape. However, the singularities from the line shape of each isotope are well-separated and spectral simulation is usually straightforward. When (iii) 14 MHz < $^{49}C_Q$ < 25 MHz, then the static ^{49}Ti line shape is accurately recorded by normal pulsed echo methods meaning that the complete NMR parameters can still be determined. However, the ^{47}Ti line is now too broad (>200 kHz) to be fully reproduced and appears as some broad underlying, usually ill-defined intensity with no clear singularities. Once (iv) $^{49}C_Q$ > 25 MHz, pulsed methods with typical probes cannot record the line shape without significant distortion in normal FT operation even with an echo. Other methods such as stepping the frequency and carrying out a point-wise acquisition to map out the line are then required.

The line shapes obtained were simulated by first considering the better-defined resonance. With the broad lines observed here and low isotopic abundance, the signal-to-noise for the complete spectrum is not always high but the singularities of at least one of the line shapes are often well-defined and allow the NMR parameters to be accurately extracted. The best fit parameters for this resonance were taken, and the C_Q was scaled by a factor of 0.8179 (^{47}Ti → ^{49}Ti) with a shift difference of 267 ppm to simulate the other isotope. If the line from this isotope was sufficiently well-defined, a simulation was accepted if it gave a good reproduction of the line as judged by eye and subtraction. It should be noted that in many cases for the broader ^{47}Ti line all that can be observed is some broad underlying intensity and not any of the singularities. In the simulations, the complete ^{47}Ti line is often shown so that the extent of this resonance as compared to the underlying intensity can be appreciated but this is not a fit to the data. In estimating the errors, the values quoted are the limits at which a significant discrepancy was noted between the simulation and the experimental line shape.

An advantage of observing both isotopes when good line shapes can be obtained for both resonances is that the presence of CSA could be determined since simulating the second isotope using only the quadrupole interaction did not provide a good fit if CSA made a significant contribution to the line shape. Similarly, in some cases, the ^{49}Ti resonance did not scale between different fields as expected considering only the quadrupole interaction. If C_Q was small enough, MAS was employed to narrow the resonance and remove the CSA, allowing the quadrupole interaction to be deduced. Then, by going back to the static data and using the quadrupole parameters from the MAS data, the CSA can be deduced. To confirm the CSA, variable field data were sometimes collected as the second-order quadrupolar and CSA scale oppositely with magnetic field. With the two isotopes, there is effectively an internal calibration since the second-order quadrupole interaction is different for the two nuclei but the CSA will be the same. Including CSA in the static line shape adds five more variables to the simulation: the span, Ω, and the skew, κ, of the CS tensor and the three angles that define the relative orientation of the two tensors.[29]

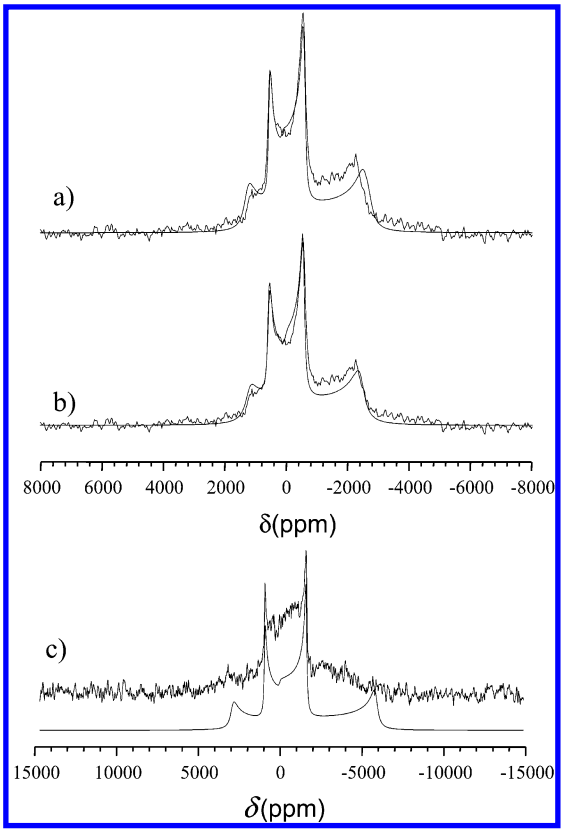

Figure 1. Static 14.1 T titanium NMR spectra of $PbTiO_3$ along with simulations (a) without and (b) with a CSA contribution (it is assumed that the tensors are aligned) and (c) $ZnTiO_3$ along with a spectral simulation.

If C_Q can be obtained by MAS (i.e., it is small enough for the line shape to narrow), then fewer parameters have to be varied. In the cases where the quadrupolar parameters could not be determined independently, it was assumed that the two tensors were coincident initially and this was confirmed by the resultant simulation. In the compounds studied here, both tensors were axially symmetric and assuming coincidence gave a good estimate of the CS parameters.

B. Spectra. B.1. TiO_6-Containing Materials. The new NMR data presented here along with that previously collected from perovskite- and ilmenite-structured $ATiO_3$ compounds are summarized in Table 1 for comparison. Some of our previous titanium NMR data was reexamined since it became clear that in some compounds CSA makes a significant contribution to the static line shape, particularly at 14.1 T. For $PbTiO_3$ fitting, the ^{49}Ti resonance assuming only second-order quadrupolar broadening gave a $^{47}C_Q$, which was too large to fit the spectrum (Figure 1a) indicating that there is a CSA contribution to the line shape. It was not possible to spin fast enough to narrow the spectrum nor to record a spectrum at one of the lower fields available to us because the quadrupolar broadening was too great. However, the similar magnetic moments of the two isotopes means that CSA will be the same for both and the scale factor for C_Q between them is accurately known. Using an axial CSA contribution of 180 ppm, a good simulation of the complete titanium spectrum was obtained (Figure 1b). Note that although CSA clearly alters the spectrum the effect on the shift and quadrupole parameters is small, and the shift is the same to within experimental error while C_Q is decreased by 5%.

There have been several reports of titanium NMR from single crystals of $BaTiO_3$ with $^{49}C_Q$ values of 3.65, 3.78, and 4.03 MHz.[18−20] A recent powder study of three different samples of

$BaTiO_3$ gave static NMR spectra all of which were consistent with $C_Q = 3.7 \pm 0.1$ MHz.[22] Bastow reported a CSA contribution of ~40 ppm to a single crystal rotation pattern.[19] Measurements on a powder sample recrystallized to remove the strain gave $^{49}C_Q = 3.77$ MHz and a span for the CS tensor of 40 ± 5 ppm.[48] The values obtained here of C_Q and the span of the CS tensor (Table 1) for our sintered $BaTiO_3$ powder are significantly different from these values. The differences greatly exceed the errors, as do the differences between the single crystal measurements. $BaTiO_3$ is an example of a perovskite that can exhibit ferroelastic strain, which is dependent on both the preparation method and the history of the sample. Local strain will couple to the titanium displacement, and these local strain effects may be large enough that the variations in local structure are sufficient to affect the NMR interactions at the titanium site.

$ZnTiO_3$ contained a small amount (~5%) of Zn_2TiO_4, but as the impurity was made in a separate experiment as a single phase sample, subtraction was straightforward leaving only the signal from $ZnTiO_3$ (Figure 1c). This spectrum is typical of one with a large quadrupole interaction, showing mainly a ^{49}Ti resonance with well-defined singularities, from which the quadrupole interaction and isotropic chemical shift can be deduced. It should be noted that although the spectrum is quite noisy as a result of the breadth of the line, the noise does not prevent extraction of the interaction parameters. In the simulation, the broader ^{47}Ti resonance is also shown (which is not a fit). The spectrum shows that only some broad underlying intensity can be observed from the much wider ^{47}Ti resonance, no features such as the singularities are present because of a combination of excitation and response of the probe over this broad frequency range. Other perovskites collected included that of the unusual A site-substituted compound $Na_{0.5}Bi_{0.5}TiO_3$. The possibility of Na,Bi disorder on the A site means that there is some distribution of environments resulting in the distinct singularities of the quadrupolar line shape being washed out. An estimate of the quadrupole interaction parameters was made by constraining η to be zero since the crystal structure determination indicates that titanium is in a site of axial symmetry. $CoTiO_3$ shows a large shift of ~2500 ppm from the region normally associated with the perovskites due to the transferred hyperfine field from the unpaired electrons on the cobalt.

Most A_2TiO_4 compounds also contain TiO_6 units, and some of these also have been studied. Zn_2TiO_4 did not show any distinct singularities, but the general form of the ^{49}Ti component of the line suggests a relatively high η (Table 1). The Sr_2TiO_4 structure contains a single titanium site of axial symmetry. This was another compound where the two isotopes could not be simultaneously fitted by the quadrupole interaction alone with the parameters simply scaled between them, suggesting that CSA effects are again important. Because $^{49}C_Q$ is <5 MHz, MAS at 14.1 T can narrow the ^{49}Ti resonance and remove CSA allowing $^{49}C_Q$ to be determined. In the MAS spectrum in Figure 2a, the ^{49}Ti resonance has a distinct line shape but the ^{47}Ti resonance is only observable as a broad, more poorly defined line. The simulation shows the ^{47}Ti line shape, but this is not a fit. Fitting static data at 14.1 T (Figure 2b) and 8.45 T (Figure 2c) was not possible by simply scaling the quadrupole interaction. Even though the ^{47}Ti line shape is quite noisy at 8.45 T, the negatively shifted singularity is sufficiently accurately determined to constrain the CSA. From the set of data shown in Figure 2, the span of the CS tensor can be estimated (by assuming that the tensors are aligned) as 120 ± 10 ppm.

Several other compounds containing TiO_6 units have been studied for the first time by ^{47,49}Ti NMR including Na_2TiO_3, Li_2TiO_3, and $Bi_2Ti_2O_7$ (Table 1). $Y_2Ti_2O_7$ provides a challenge since it contains a highly distorted TiO_6 unit. The spin−echo data at 14.1 T show a quite strongly peaked spectrum in the center of the spectral range (Figure 3a). The singularities of the ^{49}Ti component are observable at ~2500 and ~−4000 ppm, but they are much weaker in intensity than expected relative to the center of the spectrum for a classical quadrupole line shape.[9] However, this is simply a reflection that for such a broad line (~250 kHz for the ^{49}Ti resonance), distortions caused by the probe response are significant. If the line shape is recorded by stepping the frequency (Figure 3d), then the amplitudes of the singularities become closer to the values expected for a second-order quadrupole line shape. An alternative method for obtaining a closer representation of the true line shape is to correct for the probe response. The probe response was approximated by taking a Gaussian function halfwidth 160 kHz. Then, the signal was multiplied by (1/amplitude of the Gaussian) over the frequency range ±100 kHz with the center multiplied by 0.5. It can be seen by comparing Figure 3a,b that this procedure improves the line shape. This approach is only really necessary on the broadest lines observed here (≥200 kHz), and it also degrades S/N so it has not been generally applied in this work. It should be noted that even for the distorted line shape (Figure 3a), the positions of the singularities can still be accurately measured and hence the quadrupole interaction estimated. If only the singularities are seen and not the detailed line shape, then η can only be approximately determined. The efg reported for $Y_2Ti_2O_7$ ($C_Q = 24$ MHz) is the largest observed by solid state NMR for titanium to date.

The effectiveness of the QCPMG sequence in acquiring Ti data was examined for a number of samples with most success for $MgTiO_3$. The conventional echo spectrum (Figure 4a) shows

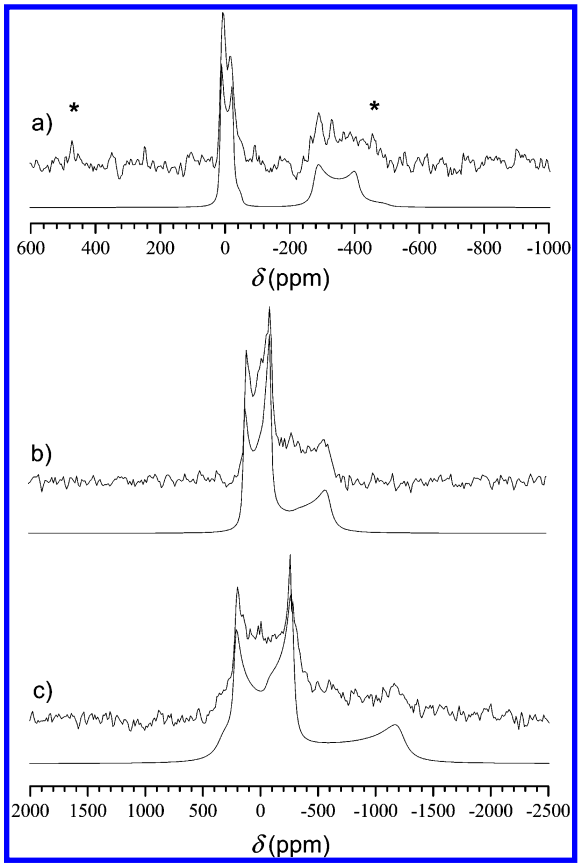

Figure 2. Titanium NMR spectra of Sr_2TiO_4 MAS (a) at 14.1 T and static (b) at 14.1 and (c) 8.45 T, along with the corresponding simulations.

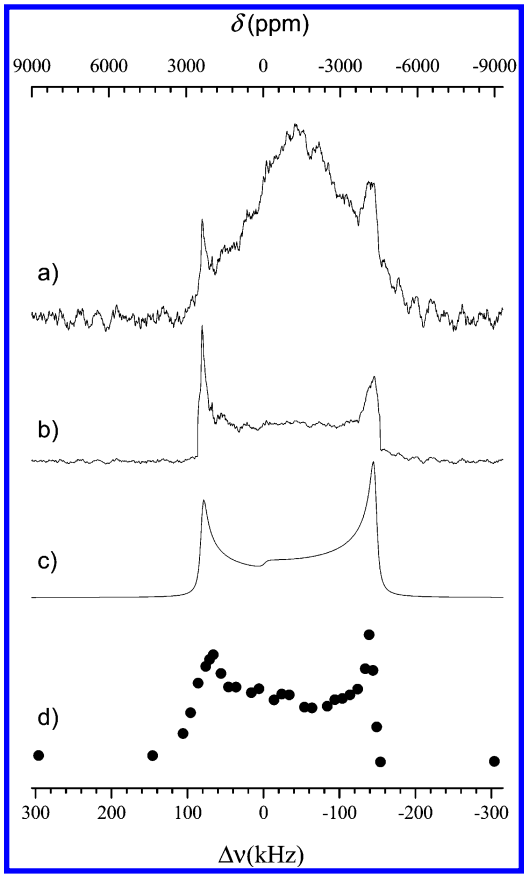

Figure 3. Titanium NMR spectra of $Y_2Ti_2O_7$ at 14.1 T showing (a) static pulse echo, (b) after correction for probe response, (c) simulation of the ^{49}Ti component, and (d) a stepped frequency point by point acquisition.

clearly the ^{49}Ti singularities. The effects of probe response can be seen as the intensity at the center of line shape is greater than would be expected for an undistorted line shape. The spectrum obtained from FT of the complete echo train (Figure 4b) shows a much broader response with a better ^{49}Ti line shape, and the up-frequency singularity of the ^{47}Ti line shape is also now visible. The intensity envelope traced out by this so-called spikelet spectrum matches that obtained by FT of the echoes all summed together (Figure 4c). In all cases, for this material, none of these approaches can capture the low-frequency singularity of ^{47}Ti at more than 200 kHz ($^{49}C_Q$ = 15.5 MHz) from the central frequency. However, the ^{49}Ti resonance is sufficiently well-defined that the ^{47}Ti line is not required in the simulation. It was also found that the QCPMG approach was not universally applicable to the titanium compounds examined here. The differing pulse responses of the two titanium isotopes, because of their different spins, means that the sequence cannot refocus each isotope equally effectively and this often leads to phase distortions in the spectra. Also, the relaxation times need to be favorable to allow formation of a long echo train.

Our titanite samples ($CaTiSiO_5$) all contained a small amount of $CaTiO_3$ (<5%), but because the spectrum from this phase had been accurately recorded independently, it was easily subtracted to produce the spectrum from titanite. In this static spectrum (Figure 5a), the ^{49}Ti component is accurately recorded, with the line shape well enough defined to extract the interaction parameters. The ^{47}Ti resonance is observable as some broad, smooth underlying intensity, which the simulation shows extends over ∼9000 ppm (∼300 kHz). The data shown agree with titanium being in a site of axial symmetry.

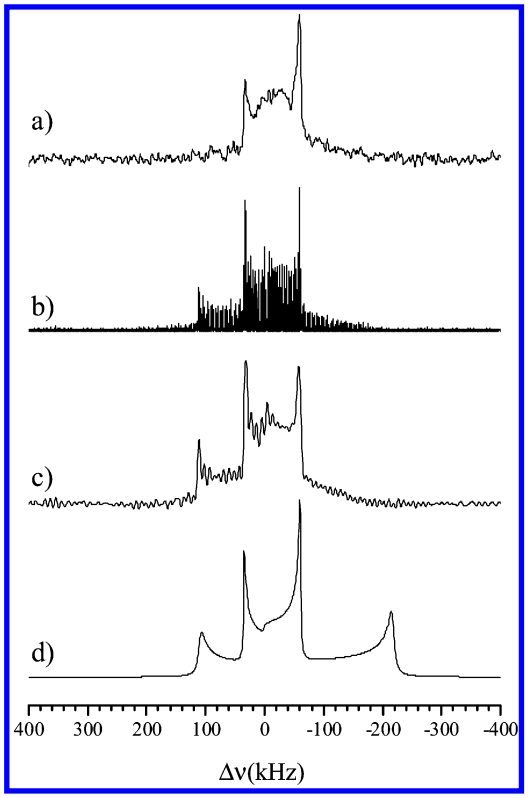

Figure 4. Titanium NMR spectra of $MgTiO_3$ collected at 14.1 T using (a) direct spin−echo, (b) Fourier transformation of the QCPMG echo train, (c) Fourier transformation of the echoes once the echoes have been summed, and (d) a simulation of the spectrum.

$Ca_4Ti_3O_{10}$ provides a challenge in that it contains two distinct titanium sites in the ratio 2:1 with significantly different structural distortions. The static spectrum has sharp components from the less distorted site that are apparent for both ^{47}Ti and ^{49}Ti (Figure 5c). The ^{49}Ti resonance from the second site completely overlaps and extends at both high and low frequency beyond that from the other site, and its singularities can be observed, but the ^{47}Ti component from this site only produces some weak, broad underlying intensity. The quadrupole interaction is small enough for the spectrum to be narrowed by spinning at 16 kHz. The overall signal is much weaker because of the much smaller sample that must be used to allow spinning at this speed; hence, the spectrum is somewhat noisy. Using the parameters deduced from the static spectrum, a good simulation of the MAS data can be obtained. The MAS data resolve the two isotopes completely (Figure 5b, i.e., the signal from the narrower resonance), but the two distinct sites are much more poorly resolved by ^{49}Ti here than in the static data. The poorer resolution for the ^{49}Ti in the MAS NMR data is because the shift difference is only ∼5 ppm so that the two narrowed ^{49}Ti lines more strongly overlap than in the static data. The quadrupole interaction is the better discriminator between these two sites producing more pronounced differences between the lines in the static spectrum.

In crystalline materials, the lower coordinations TiO_5 and TiO_4 are much less common, but some examples have been synthesized and their NMR parameters determined as part of this study. The results are summarized in Table 2. In $NaTiSiO_5$ and $LiTiSiO_5$, the TiO_5 unit has four equivalent oxygens and one distinct Ti−O bond, which manifests itself as an $\eta = 0$ titanium site. $K_2Ti_2O_5$ has a relatively large shift. Susceptibility measurements show that the sample has a significant paramagnetic contribution, which could come from either each titanium

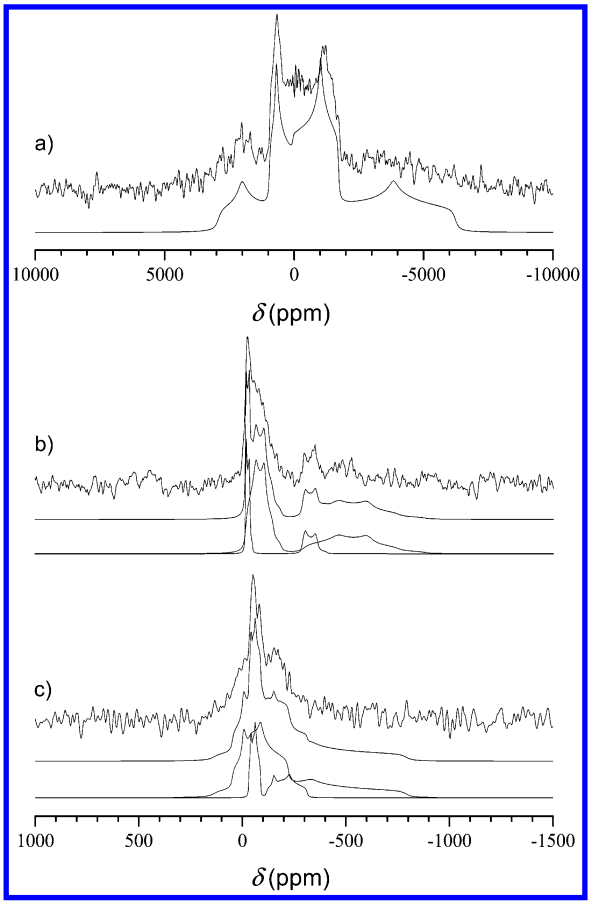

Figure 5. Titanium 14.1 T NMR spectra of (a) $CaTiSiO_5$ static together with a simulation and of $Ca_4Ti_3O_{10}$ (b) MAS and (c) static along with the simulation showing the two inequivalent TiO_6 sites.

TABLE 2: ^{49}Ti NMR Interaction Parameters for TiO_5 and TiO_4 Units in Some Crystalline Materials

compd	TiO_x coord	structural ref	C_Q (MHz)	η	δ_{iso} (ppm)
$CsAlTiO_4$	4	49	7.9 ± 0.1	1.00 ± 0.05	105 ± 15
Na_4TiO_4	4	24	18.5 ± 0.3	0.55 ± 0.05	195 ± 20
Li_4TiO_4	4	50	16.9 ± 0.3	0.00 ± 0.05	-200 ± 25
Ba_2TiO_4	4	51	12.1 ± 0.2	0.00 ± 0.05	210 ± 20
Na_2TiSiO_5	5	52	18.2 ± 0.3	0.00 ± 0.05	150 ± 20
Li_2TiSiO_5	5	53	13.2 ± 0.2	0.00 ± 0.05	130 ± 10
$KNaTiO_3$	5	53	8.9 ± 0.1	0.30 ± 0.05	80 ± 10
$K_2Ti_2O_5$	5	54	14.9 ± 0.2	0.20 ± 0.05	-1160 ± 30

having a small magnetic moment or a small fraction of the titanium being Ti^{3+}. These moments presumably cause the shift via the hyperfine interaction. Given that the line is not significantly broadened, this suggests that the moments are uniformly distributed favoring the explanation that each titanium has a small moment. The quadrupole interaction for these TiO_5 units is on average significantly larger than those typically recorded for the TiO_6 units, with the smallest value for TiO_5 being 8.9 MHz for $KNaTiO_3$. For the TiO_4-containing compounds, the C_Q is again typically quite large (Table 2).

C. Structural Correlations and Shift Ranges. Although ab initio calculations of NMR interactions have greatly improved in recent years, they crucially depend on the accuracy and completeness with which the crystal structure is known (e.g., see ref 55). A common alternative approach to understand and extend the application of NMR data is to develop correlations of the NMR parameters to structural factors by examining compounds whose crystallographic details are well-known. Although the efg is a long distance effect through its r^{-3}

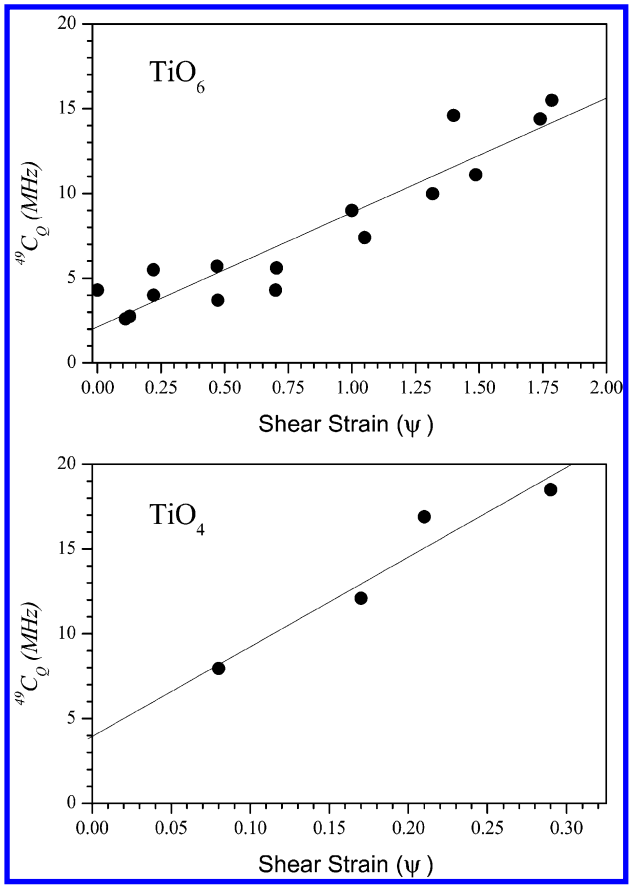

Figure 6. Correlations of the $^{49}C_Q$ against the local shear strain of the local coordination polyhedron for TiO_6 and TiO_4 units.

dependence, it is often found that efgs are dominated by local effects, so that correlations of quadrupole parameters to local structure have been very successful. Distortions in the local environment that can give rise to an efg are variations in bond lengths and angles. An extensive study by Ghose and Tsang[56] examined the quadrupole interaction of ^{27}Al in a range of materials and suggested that both the longitudinal and the shear strains of the local coordination polyhedra were good measures of the distortion that could be correlated to the quadrupole parameters. The longitudinal strain $|\alpha|$ is defined as

$$|\alpha| = \sum_i \ln\left|\frac{l_o}{l_u}\right| \qquad (2)$$

where l_o is the individual observed Ti−O bond length and l_u is the bond length of the perfect coordination polyhedron with the same volume as the coordination polyhedron of the structure. The shear strain $|\psi|$ is defined as

$$|\psi| = \sum_i |\tan(\theta_o - \theta_u)| \qquad (3)$$

where θ_o is the individual observed O−Ti−O bond angle and θ_u are the bond angles in an ideal undistorted coordination polyhedron, which is 90° for an octahedron and 109.5° for a tetrahedron. For the range of TiO_6 units measured here, there is a clear trend with C_Q increasing with $|\alpha|$ but there is considerable scatter so that the correlation is not strong. The shear strain provides a good correlation for TiO_6 (Figure 6a) and TiO_4 (Figure 6b) although there are inevitably fewer points for TiO_4. The correlations deduced for TiO_6 (with regression parameter $R = 0.95$, $n = 18$) and TiO_4 ($R = 0.96$, with $n = 4$)

are

$$^{49}C_Q\,(\mathrm{MHz}) = 1.9 + 6.9|\psi| - \mathrm{TiO_6}$$

$$^{49}C_Q\,(\mathrm{MHz}) = 3.9 + 53|\psi| - \mathrm{TiO_4} \qquad (4)$$

The correlations do not pass through the origin. This apparently indicates that with no distortion there is an efg, which may at first sight seem a contradiction. However, two points should be noted here. First, the defined shear strain only relates to the local coordination polyhedron whereas the efg can arise from effects at much larger distances than this. Not passing through the origin could be indicative of a component to the efg from further away. Second, correlations to the shear strain only examine the angular distortion of the polyhedra. So, for example, in Sr_2TiO_4 (TiO_6), all of the bond angles related to the correlation are 90°. However, examining the Ti−O bond lengths, there is one shorter and one longer than the other four, which must give rise to a field gradient even though the angular distortion is zero.

For the TiO_5 sites, the equivalent of the shear strain is less obvious but Baur et al. introduced a distortion index (DI).[57] In an undistorted trigonal bipyramid, there are six apical−equatorial angles of 90°, three equatorial angles of 120°, and one apical angle of 180°. Then, the DI is defined by

$$\mathrm{DI} = \frac{\sum_{i=1}^{10} |\theta_\mathrm{u} - \theta_\mathrm{o}|}{\sum_{i=1}^{10} \theta_\mathrm{u}} \qquad (5)$$

where θ_u and θ_o are the angles in an undistorted pentagonal bipyramid and those actually observed. This DI provides a common form for describing the distortion for all of the local units. Equation 5 can be generalized so that the sum is over 12, 10, and 6 angles, respectively, for TiO_6, TiO_5, and TiO_4, with the corresponding θ_u values being 90°, (6 × 90°, 3 × 120°, 1 × 180°), and 109.5°. These correlations are shown in Figure 7 and can be seen to be equally good as correlations to the more traditional parameters used to describe distortion (TiO_6 R = 0.93, TiO_5 R = 0.77, TiO_4 R = 0.96). The equations for these correlations are

$$^{49}C_Q\,(\mathrm{MHz}) = 2.0 + 129\mathrm{DI} - \mathrm{TiO_6}$$

$$^{49}C_Q\,(\mathrm{MHz}) = 1.8 + 106\mathrm{DI} - \mathrm{TiO_5}$$

$$^{49}C_Q\,(\mathrm{MHz}) = 4.0 + 590\mathrm{DI} - \mathrm{TiO_4} \qquad (6)$$

Both of these sets of correlations are strong enough that they provide useful information on the distortion of local units in compounds where it is poorly known and can also help identify the different units. For example, in $Ca_4Ti_3O_{10}$, the structure indicates that there are two distinguishable TiO_6.[44] The TiO_6 units occur in blocks of three layers,[43] with those in the two outer layers more distorted than the site in the inner layer. The correlation would assign the more intense line in the NMR spectrum to the more distorted site, as suggested by the crystal structure. Another example of the use of the correlation is in analysis of the spectrum reported in the literature from $FeTiO_3$.[10] The correlation (eq 6) was used to estimate a value of $^{49}C_Q$ = 12.5 MHz for $FeTiO_3$. The line shape is not well-defined, but the spectrum could be simulated using this value along with some broadening and η = 0.35. Furthermore, the value from the correlation is close to that calculated using WIEN97, which gave $^{49}C_Q$ = 11.9 MHz. Ilmenite ($FeTiO_3$) is known to be antiferromagnetic at low temperature, and because spin polarization could affect the calculated efg, a WIEN calculation, which takes into account the spin ordering, was undertaken. The calculated C_Q of 13.9 MHz is ∼20% higher for the magnetic state as compared to the case when spin is neglected, with the experimental value lying between these values.

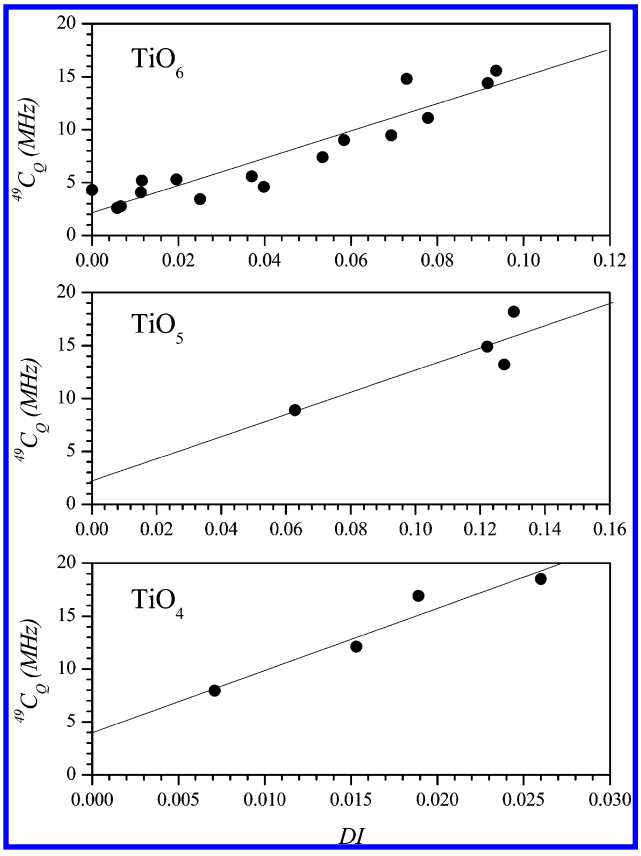

Figure 7. Correlations of the $^{49}C_Q$ against the generalized local DI for TiO_6, TiO_5, and TiO_4.

The efg in some titanates has also been examined by Catchen et al. using perturbed angular correlation spectroscopy (PACS) by implanting ^{181}Hf/^{181}Ta as the probe nucleus.[58] The efg (V_{zz}) can be derived from the experimentally measured $^{49}C_Q$ via

$$V_{zz}\,(\mathrm{V/m^2}) = 1.679 \times 10^{20} \times {}^{49}C_Q\,(\mathrm{MHz}) \qquad (7)$$

The values of the quadrupole interaction parameters deduced for the compounds that have been studied here by NMR are summarized in Table 3. The values of the efg from the PACS study are 4−8 times larger than those determined directly from the titanium NMR indicating that insertion of the PACS probe locally distorts the structure. Interestingly, all approaches tend to agree on η. The quadrupole parameters (efg and η) have also been calculated using the WIEN97 code. In most cases, the agreement between calculation and experiment for V_{zz} is very good, being within a few percent (Table 3). Similarly, for the nonaxial materials, the calculated value of η (which depends on all three components of the field gradient tensor) is in reasonable agreement with experiment. There is a significant difference between theory and experiment for the ilmenite form of $CdTiO_3$ where the discrepancy in V_{zz} is ∼35%. The larger disparity in this case is most probably due to inaccuracy in the 1932 crystal structure. The WIEN97 calculations seem to be

TABLE 3: Comparison of efgs Determined from NMR, PACS, and Ab Initio Calculations[a]

	NMR		PACS[57]		WIEN97	
sample	V_{zz}	η	V_{zz}	η	V_{zz}	η
$CdTiO_3$ perovskite	0.70 ± 0.01	0.40 ± 0.05	4.0	0.4	0.61	0.21
$CdTiO_3$ ilmenite	1.92 ± 0.02	0.10 ± 0.03	8.5	0.05	1.29	0
$PbTiO_3$	1.71 ± 0.01	0	14.0	0.1	1.69	0
$CaTiO_3$	0.47 ± 0.02	0.75 ± 0.06			0.44	0.86
(^{43}Ca site)	2.13 ± 0.03	0.70 ± 0.07			1.90	0.69
$MgTiO_3$	2.68 ± 0.01	0			2.66	0
(^{25}Mg site)	0.38 ± 0.03	0.10 ± 0.05			0.37	0
$FeTiO_3$	2.1 ± 0.2	0.35 ± 0.10			2.0, 2.5[b]	0.

[a] V_{zz} is in units of 10^{21} V/m^2. [b] Calculated assuming antiferromagnet spin ordering (see text) for Mg experimental data taken from ref 22.

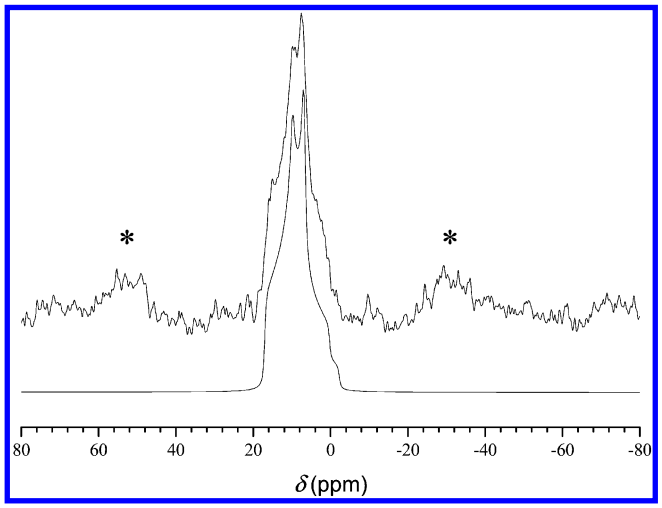

Figure 8. Experimental ^{43}Ca MAS NMR data from $CaTiO_3$ recorded at 14.1 T together with a spectral simulation; * indicates spinning sidebands.

able to predict V_{zz} to within a few percent; however, the efg is very sensitive to the structure. Thus, comparison of the calculation and experimental data provides a good test of the quality of that structure. It is clear from these data that the insertion of a probe nucleus in PACS considerably distorts the site it enters, significantly increasing the actual field gradient. Alternatively, the probe nucleus may not have substituted directly for titanium going instead to another site. A similar conclusion was recently reached by comparing the quadrupole interaction parameters for the difference phases of $BaTiO_3$ deduced from NMR and PACS,[48] where it was found that PACS gave a greatly increased quadrupolar interaction as compared with NMR.

WIEN97 calculations have also been carried out for ^{25}Mg in $MgTiO_3$ and ^{43}Ca in $CaTiO_3$ (Table 3). For ^{25}Mg in $MgTiO_3$, there is very good agreement between the V_{zz} and η deduced from the NMR data[22] and the calculated value. ^{43}Ca is another low-γ quadrupole nucleus that has been little studied to date but that high magnetic fields are making more accessible.[7] Here, the ^{43}Ca MAS NMR spectrum is reported from $CaTiO_3$ for the first time (Figure 8) and the second-order quadrupole line shape can be readily simulated. The interaction parameters deduced from the simulation were $C_Q = 2.15 \pm 0.03$ MHz, $\eta = 0.70 \pm 0.07$, and $\delta_{iso} = 17.2 \pm 1.0$ ppm. The WIEN97-calculated parameters are again in very good agreement with these experimentally determined values.

The chemical shift is the parameter most often used in chemistry to identify local structure from NMR. Plotting the isotropic chemical shift for ^{49}Ti against the mean TiO bond distance, it can be seen that there is a weak but definite

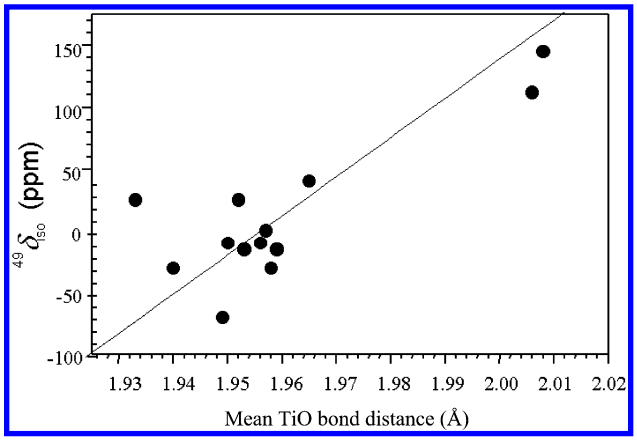

Figure 9. Isotropic chemical shift vs mean bond length for TiO_6 units.

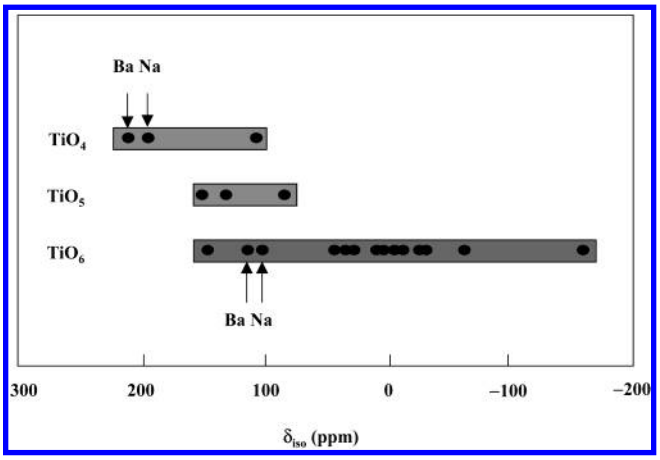

Figure 10. Isotropic chemical shift ranges of TiO_6, TiO_5, and TiO_4 units in crystalline diamagnetic compounds (including shifts of TiO_2 from ref 10).

correlation for TiO_6 units (Figure 9), with the chemical shift increasing with bond length. Similar trends are seen for TiO_5 and TiO_4, but each trend has very few data points. A key question is, on the basis of chemical shift data alone, could the titanium coordination be assigned? The shift ranges that are now observed for crystalline compounds are shown in Figure 10. The TiO_6 units cover a range in excess of 300 ppm; those of TiO_5 and TiO_4 are much more limited given the restricted number of compounds examined. It might be argued that all of the shift ranges overlap in the region of 100 ppm, which would make unambiguous assignment very difficult. However, considering factors such as the cation other than titanium, for instance, comparing different compounds containing either sodium or barium, there are shift differences of ~100 ppm between the TiO_4 and the TiO_6, and these differences are easily determined. Thus, provided the chemical composition is known, the chemical shift could provide some evidence as to the coordination of titanium.

IV. Conclusions

With the application of high applied magnetic fields (≥14.1 T), titanium NMR spectra from crystalline compounds can readily be observed. A flexible NMR approach that combines static, MAS, and, for the very widest lines, frequency-stepped experiments needs to be adopted. From the line shapes, the NMR interaction parameters could be deduced. It should be noted that in simulating static NMR data to extract the quadrupolar interaction a number of cases were found where significant (100−200 ppm) CSA is present. Thus, the analysis of static

titanium NMR data often needs to account for CSA effects especially at high magnetic fields. The efg correlates well to the structural distortion of the titanium sites for all titanium coordinations. This correlation allows the identification and assignment of different sites within the structure. The efgs determined directly by NMR do not agree with the indirectly determined values from PACS. The accuracy of calculations of the efg using the WIEN97 code is sufficiently high that where there are large discrepancies between calculation and experiment it is probable that the current crystal structure is not sufficiently accurate. The isotropic chemical shift ranges assigned to the different titanium coordinations are not well-separated. However, comparing compounds with the same cations, chemical shift differences between TiO_4 and TiO_6 of ~100 ppm exist, which are significantly greater than the errors and so may help with the identification of titanium coordination in materials where it is unknown.

Acknowledgment. HEFCE and EPSRC are thanked for funding NMR equipment at Warwick, and D.P. thanks EPSRC for partially funding a studentship. Dr. A. P. Howes is thanked for his help with the NMR measurements. Dr. M. R. Lees is thanked for the susceptibility measurements on the $K_2Ti_2O_5$. M.E.S. thanks the Royal Society and Leverhulme Trust for a senior research fellowship.

References and Notes

(1) Brinker, C. J.; Scherer, G. W. *Sol−Gel Science, The Physics and Chemistry of Sol−Gel Processing*; Academic Press: San Diego, 1990.
(2) Itoh, M.; Hattori, H.; Tanabe, K. J. *J. Catal*. **1974**, *35*, 225.
(3) Balfour, J. G. *Technological Applications of Dispersions*; Marcel Dekker: New York, 1994.
(4) Yeh, Y. C.; Tseng, T. T.; Chang, D. A. *J. Am. Ceram. Soc.* **1989**, *72*, 1472.
(5) Fujishima, A.; Honda, K. *Nature* **1972**, *37*, 238.
(6) O'Regan, B.; Grätzel, M. *Chem. Rev.* **1995**, *95*, 49.
(7) Smith, M. E. *Ann. Rep. NMR Spectrosc.* **2001**, *43*, 121.
(8) Pyykko, P. *Mol. Phys.* **2001**, *99*, 1617.
(9) Smith, M. E.; van Eck, E. R. H. *Prog. NMR Spectrosc.* **1999**, *34*, 159.
(10) Bastow, T. J.; Gibson, M. A.; Forwood, C. T. *Solid State Nucl. Magn. Reson.* **1998**, *12*, 201.
(11) Labouriau, A.; Earl, W. L. *Chem. Phys. Lett.* **1997**, *270*, 278.
(12) Kanert, O.; Kolem, H. *J. Phys. C* **1988**, *21*, 3909.
(13) Bastow, T. J.; Doran, G.; Whitfield, H. J. *Chem. Mater*. **2000**, *12*, 436.
(14) Gervais, C.; Smith, M. E.; Pottier, A.; Jolivet, J.-P.; Babonneau, F. *Chem. Mater*. **2001**, *13*, 462.
(15) Dec, S. F.; Davis, M. F.; Maciel, G. E.; Bronnimann, C. E.; Fitzgerald, J. J.; Han, S. *Inorg. Chem*. **1993**, *32*, 955.
(16) Bastow, T. J.; Whitfield, H. J. *Chem. Mater*. **1999**, *11*, 3518.
(17) Forbes, C. E.; Harwood, W. B.; Cipollini, N. E.; Lynch, J. F.; *J. Chem. Soc., Chem. Commun.* **1987**, 433.
(18) Sommer, R.; Maglione, M.; van der Klink, J. J. *Ferroelectrics* **1990**, *107*, 307.
(19) Bastow, T. J. *J. Phys. Condens. Matter* **1989**, *1*, 4985.
(20) Kanert, O.; Schulz, H.; Albers, J. *Solid State Commun*. **1994**, *91*, 465.
(21) Tunstall, D. P.; Todd, J. R. M.; Arumugam; S.; Dai, G.; Dalton, M.; Edwards, P. P. *Phys. Rev. B* **1994**, *50*, 16541.
(22) Padro, D.; Dupree, R.; Howes, A. P.; Smith, M. E. *Solid State Nucl. Magn. Reson.* **2000**, *15*, 231.
(23) Bastow, T. J.; Botton, G. A.; Etheridge, J.; Smith, M. E.; Whitfield, H. J. *Acta Crystallogr. A* **1999**, *55*, 127.
(24) Kissel, J.; Hoppe, R. *Z. Anorg. Allg. Chem.* **1990**, *582*, 103.
(25) Larsen, F. H.; Jakobsen, H. J.; Ellis, P. D.; Nielsen, N. C. *J. Magn. Reson.* **1998**, *131*, 144.
(26) Larsen, F. H.; Skibsted, J.; Jakobsen, H. J.; Nielsen, N. C. *J. Am. Chem. Soc*. **2000**, *122*, 7080.
(27) Massiot, D.; Fayon, F.; Capron, M.; King, I.; Le Calve, S.; Alonso, B.; Durand, J.-O.; Bujoli, B.; Gan, Z.; Hoatson, G. *Magn. Reson. Chem.* **2002**, *40*, 70.
(28) Blaha, P.; Schwarz, K.; Luitz, J. *Wien 97, A Full Potential Linearised Augmented Plane Wave Package for Calculating Crystal Properties*; Karl-Heinz Schwarz, Technische Universität: Wien, Austria, 1999.
(29) MacKenzie, K. J. D.; Smith, M. E. *Multinuclear Solid State NMR of Inorganic Materials*; Pergamon Press: Oxford, 2002.
(30) Koopmans, H. J. A.; Van de Velde, G. M. *Acta Crystallogr. C* **1983**, *39*, 1323.
(31) Posnjak, E.; Barth, T. F. *Zeit. Kristal.* **1934**, *88*, 271.
(32) Sasski, S.; Prewitt, C. T.; Bass, J. D. *Acta Crystallogr. C* **1987**, *43*, 1668.
(33) Weschler, B. A.; Dreele, R. B. *Acta Crystallogr. B* **1989**, *45*, 542.
(34) Golochansky, A.; Kim, H. T.; Kim, Y. *J. Korean Phys. Soc*. **1998**, *32*, S1167.
(35) Jones, G. O.; Thomas, P. A. *Acta Crystallogr. B* **2002**, *58*, 168.
(36) Kidoh, K.; Tanaka, K.; Marumo, F.; Takei, H. *Acta Crystallogr. B* **1984**, *40*, 92.
(37) Shirane, G.; Pepkinsky, R. *Acta Crystallogr*. **1956**, *9*, 131.
(38) Harada, J. *Acta Crystallogr. A* **1970**, *26*, 336.
(39) Lukaszewicz, K. *Angew. Chem.* **1959**, *33*, 239.
(40) Millard, R. L.; Peterson, R. C.; Hunter, B. K. *Am. Mineral.* **1995**, *80*, 885.
(41) Wechsler, B. A.; von Dreele, R. B. *Acta Crystallogr. B* **1989**, *45*, 542.
(42) Hill, W. Masters Thesis, NSW Institute of Technology, Sydney, Australia 1982.
(43) Dittrich, G.; Hoppe, R. *Z. Anorg. Allg. Chem.* **1969**, *371*, 306.
(44) Elcombe, M. M.; Kisi, E. H.; Hawkins, K. D.; White. T. J.; Goodman, P.; Matheson, S. *Acta Crystallogr. B* **1991**, *47*, 305.
(45) Chtoun, E.; Hanebali, L.; Garnier, P., Kiat, J. M. *Eur. J. Solid State Chem.* **1997**, *34*, 553.
(46) Shimada, S.; Kodiara, K.; Matsushita, T. *J. Cryst. Growth* **1977**, *41*, 317.
(47) Kek, S.; Arroyo, M.; Bismayer, U.; Schmidt, C.; Eichhorn, K.; Krane, H. G. *Zeit. Kristall.* **1997**, *212*, 9.
(48) Bastow, T. J.; Whitfield, H. J. *Solid State Commun.* **2001**, *117*, 483.
(49) Peres, V.; Fabry, P. Genet, F.; Dehandt, P. *J. Eur. Ceram. Soc.* **1994**, *13*, 403.
(50) Gunawardane, R. P.; Fletcher, J. G.; Dissanayake, M. A. K. I.; Howie, R. A.; West, A. R. *J. Solid State Chem.* **1994**, *112*, 70.
(51) Guenther, J. R.; Jameson, G. B. *Acta Crystallogr. C* **1984**, *40*, 207.
(52) Egorov-Tismenko, Y. K.; Simonov, M. A.; Belov, N. V. *Dokl. Akad. Nauk. SSSR* **1978**, *240*, 78.
(53) Werthmann, R.; Hoppe, R. *Zeit. Anorg. Allg. Chem.* **1985**, *523*, 54.
(54) Andersson, S.; Wadsley, A. D. *Acta Chem. Scand*. **1961**, *15*, 663.
(55) Bull, L. M.; Bussemer, B.; Anupõld, T.; Reinhold, A.; Samoson, A.; Sauer, J.; Cheetham, A. K.; Dupree, R. *J. Am. Chem. Soc.* **2000**, *122*, 3510.
(56) Ghose, S.; Tsang, T. *Am. Mineral.* **1973**, *58*, 748.
(57) Baur, W. H. *Acta Crystallogr. B* **1974**, *30*, 1195.
(58) Catchen, G. L.; Wukich, S. J.; Spaar, D. M.; Blaszkiewicz, M. *Phys. Rev. B* **1990**, *42*, 1885.